INSTITUT DE FRANCE
Académie des sciences

Comptes Rendus

Chimie

Peng Wang, Ziqi Wang, Zhongqing Yang, Zhilei Liu, Jingyu Ran and Mingnv Guo

Selective catalytic and kinetic studies on oxydehydrogenation of ethane with CO_2 over lanthanide metal catalysts

Volume 23, issue 1 (2020), p. 33-46

Published online: 6 May 2020

https://doi.org/10.5802/crchim.4

Les Comptes Rendus. Chimie *sont membres du*
Centre Mersenne pour l'édition scientifique ouverte
www.centre-mersenne.org
e-ISSN : 1878-1543

Comptes Rendus
Chimie
2020, 23, nº 1, p. 33-46
https://doi.org/10.5802/crchim.4

Full paper / *Mémoire*

Selective catalytic and kinetic studies on oxydehydrogenation of ethane with CO_2 over lanthanide metal catalysts

Peng Wang [a, b], Ziqi Wang [a, b], Zhongqing Yang [a, b]*, Zhilei Liu [a, b], Jingyu Ran [a, b]* and Mingnv Guo [c]

[a] Key Laboratory of Low-Grade Energy Utilization Technologies and Systems, Ministry of Education of China, Chongqing University, Chongqing, 400044, China

[b] School of Energy and Power Engineering, Chongqing University, Chongqing, 400044, China

[c] School of Mechanical and Power Engineering, Chongqing University of Science and Technology, Chongqing, 401331, China.

E-mails: zqyang@cqu.edu.cn (Z. Yang), ranjy@cqu.edu.cn (J. Ran).

Abstract. Single metal catalysts with different active components (La, Sm, Ce) and La loadings (5%, 10%, 15%) were prepared. Oxydehydrogenation of C_2H_6 with CO_2 over the above catalysts was studied by catalyst activity experiments and characterization tests. The results indicate that the homogeneous reaction of CO_2/C_2H_6 is the coupling of ethane pyrolysis and hydrogenolysis. Dehydrogenation has better selectivity than reforming on La/Sm/Ce-based catalysts; Sm exhibits the best catalytic activity due to carbon deposition resistance and many oxygen vacancies. C_2H_6 conversion on 10% Sm/SiO_2 is 42.75% at 700 °C, but C_2H_4 selectivity is lowest. Because of the existence of Ce^{4+}, Ce has the best C_2H_4 selectivity; it has potential to modify the catalyst, but its catalytic activity is lowest. La shows the best catalytic performance. The activation energy on 10% La/SiO_2 is 83.99 kJ/mol, C_2H_4 selectivity is 96.84% at 700 °C, and its optimum loading is between 10% and 15%.

Keywords. Ethylene, Oxidative dehydrogenation, Catalytic selectivity, Lanthanide metal, Apparent activation energy.

Manuscript received 30th August 2019, revised and accepted 31st October 2019.

Highlights

1. Ethane pyrolysis and hydrogenolysis constitute the gas-phase reaction of CO_2/C_2H_6
2. Dehydrogenation has better selectivity than reforming on La/Sm/Ce-based catalysts
3. La shows the best catalytic performance, optimum loading is between 10% and 15%
4. Ce can modify the catalyst by high C_2H_4 selectivity, because of high valence Ce^{4+}

* Corresponding authors.

1. Introduction

Ethylene is one of the most produced and essential chemical products in the world [1–3]. Oxydehydrogenation of C_2H_6 with CO_2 to C_2H_4 provides new ideas for pressing issues (energy conservation and emission reduction, green chemical industry, sustainable development) [4–12]. The reaction not only promotes the comprehensive utilization of natural gas [13], but also overcomes the shortcomings (high pollution and high energy consumption) of high-temperature pyrolysis of petroleum to ethylene [14, 15]. In addition, it consumes carbon dioxide and reduces greenhouse gas emissions [16,17]. Oxydehydrogenation of C_2H_6 with CO_2 not only has great practical significance for solving the energy crisis, but also mitigates the impact of the greenhouse effect on the global ecological environment [18,19]. The main reaction paths of catalytic oxidized ethane with CO_2 include reforming (reaction 1) and dehydrogenation (reaction 2).

$$C_2H_6 + 2CO_2 \rightarrow 4CO + 3H_2 \quad (1)$$

$$C_2H_6 + CO_2 \rightarrow C_2H_4 + CO + H_2O \quad (2)$$

Lanthanide metal oxides have a special outer electronic structure, and are usually used as a carrier, promoter and active component. They have an important influence on the C_2H_6 conversion pathway. Valenzuela *et al.* [20,21] studied a CeO_2-based catalyst and found that the addition of Ce^{2+} reduced the catalytic activity, but C_2H_4 selectivity could be increased to 91%, C_2H_4 yield could reach 22%. The phase of the rare earth metal oxide would greatly affect C_2H_6 conversion and C_2H_4 selectivity. For example, in the oxidative dehydrogenation of ethane reaction system, C_2H_4 selectivity on pure La_2O_3 catalyst was 48.2%, but C_2H_4 selectivity on La_2O_2/CO_2^{3-} catalyst was only 6.7%. For the CeO_2-based catalyst, the addition of Na promoter could improve the reaction performance, and C_2H_4 selectivity could reach 70%. It indicates that rare earth oxides are a good catalyst for the oxidation and dehydrogenation of C_2H_6 to C_2H_4. Besides, Beretta *et al.* [22] showed that C_2H_4 yield can reach 50% on Pt/Al_2O_3 catalyst at 500 °C. Lu *et al.* [23] synthesized $Al/Pd/Al_2O_3$ catalysts by atomic layer deposition method. There was low coordination number Pd active sites on Al_2O_3, and these sites were beneficial to break C–C bonds and reduce carbon deposition. C_2H_4 selectivity was 99.0% at 675 °C; it still maintained stable activity within 1800 min. Nakagawa *et al.* [24] studied the catalytic performance of various metal oxides for ethane oxidative dehydrogenation at 650 °C. The results showed that the activity of the catalyst follows the order: Ga_2O_3>V_2O_5>TiO_2>Mn_3O_4>In_2O_3>ZnO. Ga_2O_3 exhibited the highest catalytic performance. They also studied the role of CO_2 in the oxidative dehydrogenation reaction over Ga-based catalysts. It was found that the catalytic activity of Ga_2O_3/TiO_2 increased with the increase of CO_2 partial pressure, indicating that CO_2 could inhibit carbon deposition, ethylene re-adsorption and promotion of desorption [25]. Koirala *et al.* [26] studied different loadings of Ga_2O_3/TiO_2 catalysts. It was found that the acid concentration decreased and the yield of ethylene increased with the increase of Ga loading between 0 and 10 wt% Ga. However, higher loadings of Ga would reduce the catalytic performance; it was due to the severe carbon deposition caused by too acidic surface. Krylov *et al.* [27] studied the oxidative dehydrogenation of alkanes (C_1–C_7) with CO_2 on different supports (Fe_2O_3, Cr_2O_3, MnO_2, etc.). MnO_2 exhibited the highest activity. Toth *et al.* [28] found that different oxide supports could regulate the reaction pathway. They found that Au/CeO_2 and Au/ZnO were beneficial to the reforming reaction, and Au/TiO_2 was beneficial to oxidative dehydrogenation. Oxidized diamond as an efficient support played a significant role in oxydehydrogenation of C_2H_6 with CO_2 to C_2H_4 over Cr_2O_3-loaded catalyst; C_2H_4 selectivity and C_2H_4 yield were 87.7% and 22.5%, respectively, at 650 °C [29]. Wang *et al.* [30] found that $LiCl/SiO_2$ exhibited the highest C_2H_6 conversion and C_2H_4 yield; C_2H_6 conversion and C_2H_4 yield were 99% and 80%, respectively, at 600 °C. However, under certain conditions, rapid deactivation would occur. Shi *et al.* [31] found that C_2H_6 conversion and C_2H_4 selectivity were 66.5% and 99.5%, respectively, on the monolithic catalyst (5% Cr) at 750 °C. The equilibrium limit of ethane conversion was successfully surpassed by increasing temperature and reaction pressure in the PBMR. Dangwal *et al.* [32] found that C_2H_6 conversion and C_2H_4 selectivity can reach 29% and 97%, respectively, at 600 °C.

Oxydehydrogenation of C_2H_6 with CO_2 to C_2H_4 not only has great practical significance for solving the energy crisis, but also mitigates the impact of the greenhouse effect on the global ecological environ-

ment. Therefore, the single-metal catalysts with different active components of lanthanide metals and different loadings of La supported on SiO_2 were prepared by incipient wetness impregnation method. The effects of the above catalysts on oxydehydrogenation of C_2H_6 were studied by catalyst activity experiments and catalyst characterization methods (XRD, EDS and SEM).

2. Experimental section

2.1. *Catalyst preparation*

The desired lanthanide metal catalysts were prepared by incipient wetness impregnation method. The lanthanide metal catalysts required for the experiment are shown in Table 1. According to the calculation of the loading, the metal precursor (m_m) was weighed into a beaker, and an equal volume of deionized water was weighed into the glass bottle according to the pore volume and the required mass (m_s) of the carrier. The carrier (m_s) was weighed and placed in a beaker, and the precursor solution was dropped into the carrier. The impregnated catalyst was placed in the drier and dried at 100 °C for 12 h. The dried bulk catalyst was ground into a fine powder in a mortar, dispersed into a thin layer, transferred to a muffle furnace and calcined at 700 °C for 5 h. The calcined catalyst powder was compressed and shaped. Catalysts with a particle size of 40–60 mesh were screened out. The chemicals used in catalyst preparation are provided in Table S1.

2.2. *Catalyst characterization*

The characterization methods were XRD, EDS and SEM. X-ray diffraction (XRD) used a BRUCKER D8 X-ray diffractometer to have a wide-angle test, a catalyst sample (40–60 mesh) which was not less than 0.1 g was ground to 200 mesh (particle size was less than 70 μm). The test conditions were as follows: with a Cu target, the tube voltage was 40 kV, the tube current was 30 mA, the 2θ angle scan range was 10°–90°, the scan rate was 6 °/min, and the scan step was 0.02. The TESCAN VEGA3 scanning electron microscope was used in SEM and EDS tests under a vacuum. The electron gun was a tungsten filament with a voltage of 2 kV and a resolution of 20 μm.

2.3. *Catalyst activity evaluation*

The flow chart of catalyst evaluation experiment is shown in Figure 1. The catalyst activity tests used a three-channel fixed-bed catalyst evaluation system (Table S3). The catalyst particles (0.25 mL, 40–60 mesh) were placed into the middle of the reactor, the packing height was about 2 cm, both ends were blocked with quartz wool, the K-type thermocouple was placed in the reactor and contacted with quartz wool. The flow of O_2 was set to 40 mL/min. The catalyst bed was heated to 600 °C in O_2 atmosphere at a heating rate of 15 °C/min and activated for 30 min. Then the O_2 valve was closed, the carrier gas N_2 valve was opened, and its flow was set to 40 mL/min. The cooling fan was turned on to cool the bed to room temperature and purged for 30 min. Subsequently, the C_2H_6 and CO_2 valves were opened, and the reaction gases (C_2H_6, CO_2) and carrier gas (N_2) were introduced into the reactor, and the furnace was heated to the desired temperature at 15 °C/min. After reaching the predetermined temperature for 40 min, the exhaust gas was collected and the content of each gas components were analyzed in the gas chromatograph (ISQ QD-TRACE1300). The experimental details including chemicals, materials and instrumentations can be found in supplementary information.

The evaluation indexes of catalytic activity were mainly C_2H_6 and CO_2 Conversion; C_2H_4, CH_4 and CO Selectivity; and C_2H_4 and CH_4 yield. The calculation equations involved in the catalytic activity test are as follows:

$$R_{\text{conversion}} = \frac{M(R_{\text{in}}) - M(R_{\text{out}})}{M(R_{\text{in}})} \times 100\%$$
$$R = \text{C}_2\text{H}_6 \text{ or } \text{CO}_2 \quad (3)$$

$$P_{\text{selectivity}} = \frac{M(P_{\text{out}})}{M(\text{C}_2\text{H}_{6\,\text{in}}) - M(\text{C}_2\text{H}_{6\,\text{out}})} \times 100\%$$
$$P = \text{C}_2\text{H}_4 \text{ or } \text{CH}_4 \quad (4)$$

$$\text{CO}_{\text{selectivity}} = 1 - \text{C}_2\text{H}_{4\ \text{selectivity}} - \text{CH}_{4\ \text{selectivity}} \quad (5)$$

$$P_{\text{yield}} = \frac{M(P_{\text{out}})}{M(\text{C}_2\text{H}_{6\,\text{in}})} \times 100\%$$
$$P = \text{C}_2\text{H}_4 \text{ or } \text{CH}_4 \quad (6)$$

In (3)–(6): M is the molar concentration of the corresponding substance. *Conversion* is the conversion of the corresponding substance. *Selectivity* is the selectivity of the corresponding substance. *Yield* is the yield of the corresponding substance.

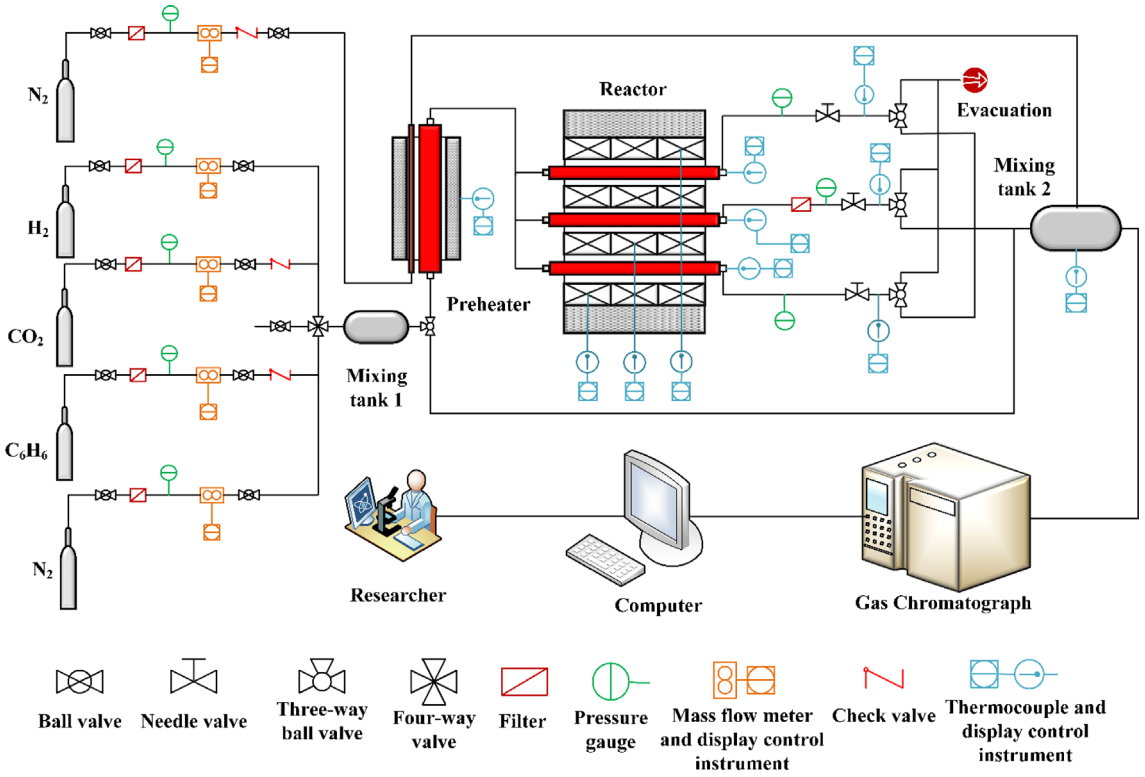

Figure 1. The flow chart of catalyst evaluation experiment.

Table 1. Lanthanide metal catalysts required for the experiment

Lanthanide metal catalysts	Active component and loading	Catalyst carrier
5% La/SiO_2	5 wt% La_2O_3	SiO_2
10% La/SiO_2	10 wt% La_2O_3	SiO_2
15% La/SiO_2	15 wt% La_2O_3	SiO_2
10% Sm/SiO_2	10 wt% Sm_2O_3	SiO_2
10% Ce/SiO_2	10 wt% CeO_2	SiO_2

2.4. *Reaction kinetics test*

The apparent activation energies of oxydehydrogenation of C_2H_6 over different lanthanide metal catalysts are calculated according to Arrhenius equation (7). The relationship between the reaction rate r and the reaction rate constant k is obtained by the reaction series theory (8). According to the principle of reaction kinetics, the expression of the catalytic reaction rate r is shown in (9).

$$k = A \cdot e^{-\frac{E}{RT}} \tag{7}$$

$$r = k \cdot C_1^{\alpha} C_1^{\beta} \cdots C_n^{\gamma} \tag{8}$$

$$r = \frac{FC \times V}{M} = \frac{FC \times \omega}{22.414 \times 60 \times 1000 \times M} \tag{9}$$

In (7), k is the reaction rate constant, A is the prefactor, E is the apparent activation energy and R is the molar gas constant. In (8), α, β and γ are reaction orders; C_1, C_2 and C_n are reactant concentrations. In (9), FC is the conversion of the reactants, ω is the gas flow rate and M is the mass of the catalyst. Equa-

tion (10) can be obtained by calculating the natural logarithm of (7). Finally, (11) can be obtained by calculating (8) and (10).

$$\ln k = \ln A - \frac{E}{RT} \tag{10}$$

$$\ln r = -\frac{E}{RT} + \ln A + \ln C_1^{\alpha} C_1^{\beta} \cdots C_{\mathrm{n}}^{\gamma} \tag{11}$$

In (11), if the linear relationship between ln r and $1/T$ can be fitted, then the slope of the line is solved. After further calculation, the apparent activation energy E can be obtained.

3. Results and discussion

3.1. *The homogeneous reaction of* CO_2/C_2H_6 *in the absence of catalyst*

In order to accurately study the catalytic performance of lanthanide metal catalysts, the occurrence of the homogeneous reaction should be avoided or minimized. The reaction temperature is the key factor to determine the degree of non-catalytic reaction. It is important that the appropriate reaction temperature is selected for studying the catalytic performance of each catalyst in this experiment [33]. Therefore, this section firstly studied the effect of temperature on the reaction of CO_2/C_2H_6 in the absence of catalysts.

The pure SiO_2 powders (0.25 mL, 40–60 mesh) without any active components were put into the quartz reaction tube. The reaction pressure was set to 0.1 MPa, the reaction gas feed ratio was $M_{CO_2/C_2H_6} = 2$, and the space velocity was 1200 h^{-1}. In order to find the temperature range with the weakest homogeneous reaction (avoid interference with catalytic reactions) and the most suitable for the catalytic reaction, the homogeneous reactions at 600 °C, 650 °C, 700 °C, 750 °C and 800 °C were studied. The experimental results are shown in Table 2.

All of experimental data is 0 when the temperature is below 600 °C; this indicates that the homogeneous reaction cannot occur at low temperature. C_2H_6 conversion increases with the increase of temperature, but CO_2 conversion is always 0, so CO_2 does not participate in the gas phase non-catalytic reaction. Therefore, it can be inferred that the essence of the homogeneous reaction is the coupling of ethane pyrolysis and ethane hydrogenolysis (reaction 12–13) [34–37]; the results of this study are similar to Xu *et al.* [38]:

$$C_2H_6 \rightarrow C_2H_4 + H_2 \tag{12}$$

$$C_2H_6 + H_2 \rightarrow 2CH_4 \tag{13}$$

A certain degree of high temperature is beneficial to the conversion process of $C_2H_6 \rightarrow C_2H_4$ in the homogeneous reaction. However, when the temperature rises to a certain value, CH_4 selectivity is higher than C_2H_4 selectivity, and C_2H_4 yield will decrease with increase of temperature [36,37]. Shi *et al.* [39] also proved that the reduction of C_2H_4 selectivity and the increase of CH_4 yield at high temperatures are caused by the promotion of side reactions at high temperatures. As the temperature increases, the probability of occurrence of corresponding side reactions increases, such as ethane cracking reaction (reaction 14):

$$C_2H_6 \rightarrow 2C(s) + 3H_2 \tag{14}$$

The increase of by-products and the further decrease of C_2H_4 selectivity are due to these side reactions [40,41]. At the same time, excessive temperature is more detrimental to the gas–solid catalytic reaction, because high temperature is more likely to produce carbon deposits. More importantly, carbon deposition is one of the important reasons that affect the catalytic performance [26,41,42].

Table 2 shows that when the temperature is 650–700 °C, there is only a weak gas-phase reaction in the reaction process. When the temperature is raised to 750–800 °C, the degree of the homogeneous reaction increases rapidly. The results are similar to Sigaeva *et al.* [40]. They have reported that the ethane pyrolysis mainly produces ethylene, and the reaction occurs rapidly at 650–900 °C. As the temperature increases, ethylene selectivity decreases, methane selectivity increases and carbon deposits are formed. In order to eliminate the influence of the homogeneous reaction when studying the catalytic performance, and avoid carbon deposition at high temperatures causing catalyst deactivation, the temperature of the gas–solid catalytic reaction should not be too high. Therefore, this paper mainly studied the catalytic performance in the temperature range of 500–750 °C.

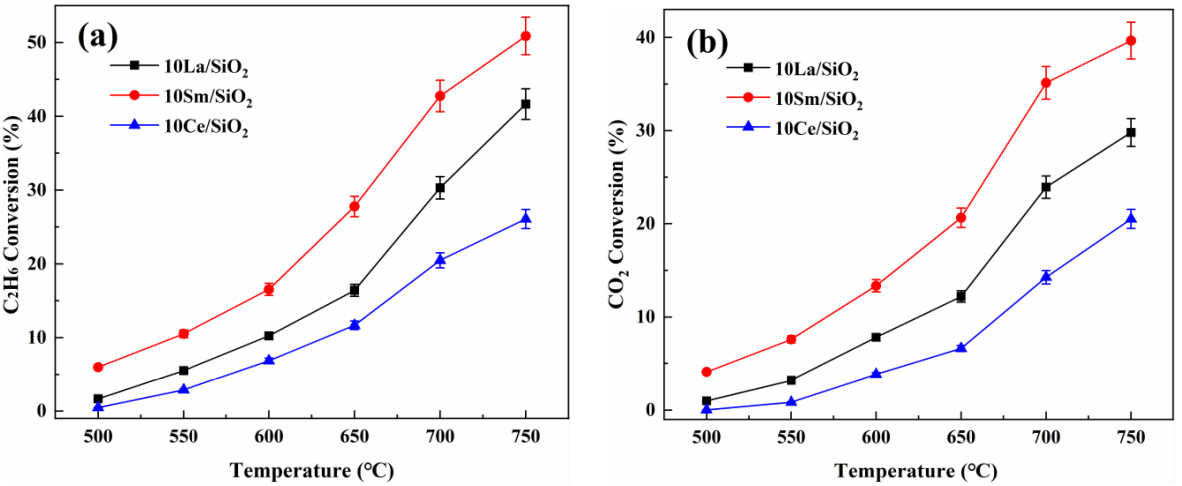

Figure 2. Effect of temperature on C_2H_6 conversion (a) and CO_2 conversion (b) on different lanthanide metal catalysts.

Table 2. Effect of temperature on the homogeneous reaction of C_2H_6/CO_2 in the absence of catalyst

Temperature (°C)	Conversion (%)		Yield (%)	Selectivity (%)		
	C_2H_6	CO_2	C_2H_4	C_2H_4	CH_4	CO
≤600	0	0	0	0	0	0
650	0.87	0	0.87	99.76	0.24	0
700	1.56	0	1.55	99.48	0.52	0
750	7.25	0	7.18	98.97	1.03	0
800	18.15	0	17.25	94.48	4.52	0

3.2. *Effect of different lanthanide metal active components on reaction performance*

In order to study the effects of different active components on the catalytic activity, 10% La/SiO_2, 10% Sm/SiO_2 and 10% Ce/SiO_2 catalysts were prepared by incipient wetness impregnation method. The catalyst particles (0.25 mL, 40–60 mesh) were placed in a quartz tube reactor. The pressure was set to 0.1 MPa, the reaction space velocity was 1200 h^{-1}, and the reaction gas feed ratio was $M_{CO_2/C_2H_6} = 2$. The effects of temperature on C_2H_6 and CO_2 conversion on different lanthanide metal catalysts are shown in Figure 2.

Figure 2 shows that C_2H_6 and CO_2 conversion on different lanthanide metal catalysts increase with an increase in temperature. 10% Ce/SiO_2 shows the lowest C_2H_6 and CO_2 conversion. At 700 °C, C_2H_6 conversion is only 20.48%, and CO_2 conversion is only 14.26%. 10% Sm/SiO_2 exhibits the best catalytic activity; its C_2H_6 conversion is 42.75% and CO_2 conversion is 35.13% at 700 °C. The catalytic activity of three lanthanide metal catalysts is in decreasing order: 10% Sm/SiO_2>10% La/SiO_2>10% Ce/SiO_2. Kennedy *et al.* [43] also got similar conclusions. They reported that the catalytic activity order of four rare earth metals for oxidative dehydrogenation of ethane is: Sm_2O_3>La_2O_3>CeO_2. According to the research results of He and Han *et al.* [44,45], the acidity and alkalinity of the catalyst are closely related to the improved catalytic activity and stability. Sm can reduce the strong acid centre of the catalyst and increase the active oxygen content, thus the carbon deposition is inhibited and the catalytic activity is improved. This is one of the reasons for the best catalytic activity of Sm. He *et al.* [46] also proposed that Sm can promote the increase in oxygen vacancies, thereby increasing the catalytic activity.

All three lanthanide metals have a high catalytic activity [43]. In the high temperature range, C_2H_6 and

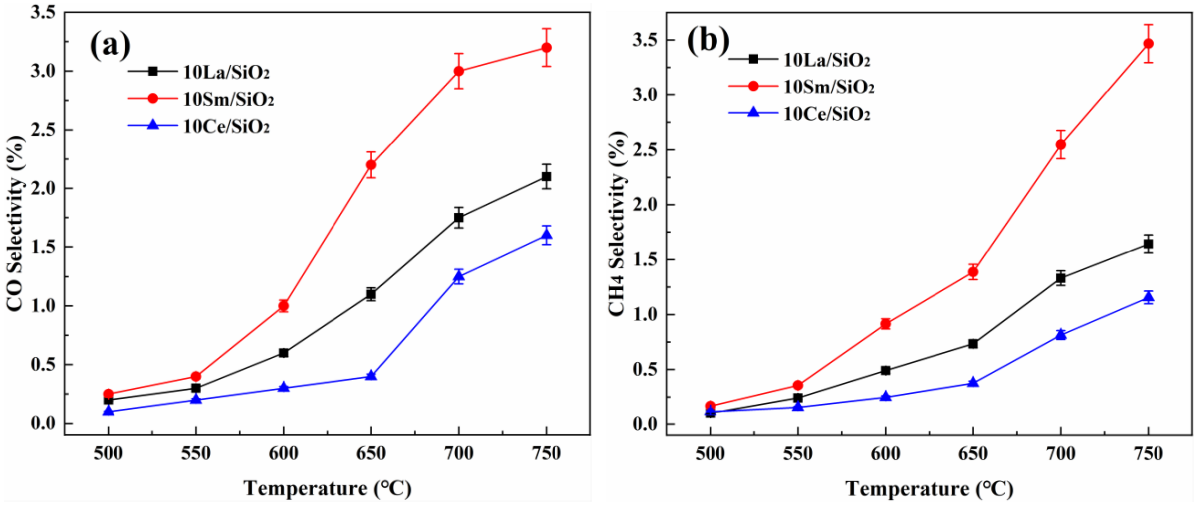

Figure 3. Effect of temperature on CO selectivity (a) and CH_4 selectivity (b) on different lanthanide metal catalysts.

CO_2 conversion increases with an increase in temperature; it shows that a high temperature is beneficial to C_2H_6 and CO_2 conversion on the lanthanide metal catalysts, but when the temperature rises to 750 °C, the increase in both conversions slows down. This indicates that high temperature promotes the formation of carbon deposition, which will cause the catalysts to be inactivated [42].

The effects of temperature on CO and CH_4 selectivity on different lanthanide metal catalysts are shown in Figure 3. CO and CH_4 selectivity on different lanthanide metal catalysts increase with the increase in reaction temperature. CO and CH_4 selectivity on the three catalysts are low; 10% Sm/SiO_2 has the best CH_4 and CO selectivity at 700°C, but it is only 2.55% and 2.87%. It can be seen that the reaction system of CO_2/C_2H_6 over lanthanide metal catalysts mainly undergoes dehydrogenation reaction instead of reforming reaction [43]. CO and CH_4 selectivity on the above three catalysts are ranked in decreasing order: 10% Sm/SiO_2>10% La/SiO_2>10% Ce/SiO_2. Although the Sm-based catalyst has the best catalytic activity, its side reaction has the best selectivity.

Figure 4 shows that C_2H_4 selectivity on different lanthanide metal catalysts decrease with the increase in reaction temperature. C_2H_4 selectivity on the above three catalysts is high. At 700 °C, C_2H_4 selectivities on 10% Ce/SiO_2, 10% La/SiO_2 and 10% Sm/SiO_2 are 97.98%, 96.84% and 94.58% respectively. C_2H_4 selectivity on the above catalysts are ranked in decreasing order: 10% Ce/SiO_2>10% La/SiO_2>10% Sm/SiO_2. Shi *et al.* [39] confirmed the key role of Ce in the conversion of ethane to ethylene. In CO_2 atmosphere, ethane is oxidized to ethylene by CeO_2, and then CO_2 oxidizes Ce^{3+} to Ce^{4+} to continue the cycle, and because of the presence of CeO_2, more ethane is converted to ethylene, thereby increasing the selectivity of ethylene [47]. This is shown in reactions 15 and 16 [20].

$$C_2H_6 + Ce^{4+} \rightarrow C_2H_4 + Ce^{3+} \quad (15)$$

$$Ce^{3+} + CO_2 \rightarrow Ce^{4+} + CO \quad (16)$$

Figure 5 shows that C_2H_4 yield on the three different lanthanide metal catalysts increases with the increase in reaction temperature. 10% Sm/SiO_2 has the lowest C_2H_4 selectivity but its C_2H_6 conversion is much higher than other lanthanide metal catalysts. Although C_2H_4 yield on 10% Ce/SiO_2 is low, it still has a high C_2H_4 selectivity at high temperatures. Many scholars who study polymetallic catalysts use this characteristic of Ce to regulate the catalyst in order to make the catalyst have high C_2H_6 conversion and C_2H_4 selectivity [48–50].

The apparent activation energy determines the ease of catalytic reaction and affects the reaction rate [51]. Therefore, it is necessary to study the apparent activation energy of different active compo-

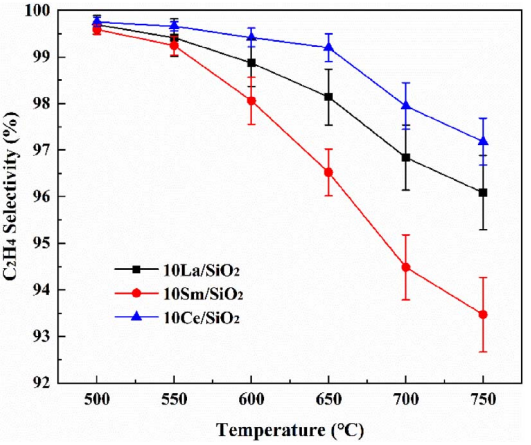

Figure 4. Effect of temperature on C_2H_4 selectivity on different lanthanide metal catalysts.

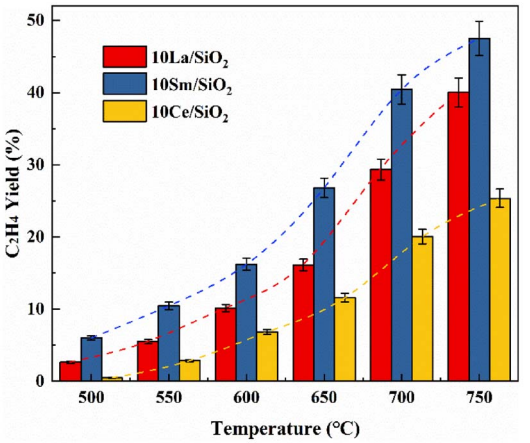

Figure 5. Effect of temperature on C_2H_4 yield on different lanthanide metal catalysts.

nent catalysts. The apparent activation energies on three different active component catalysts are shown in Figure 6.

Figure 6 shows that the activation energies of the three lanthanide metal catalysts for the catalytic reaction of CO_2/C_2H_6 are in increasing order: 10% Sm/SiO_2<10% La/SiO_2<10% Ce/SiO_2; the results are consistent with the previous catalyst activity experiments. The activation energy on 10% Sm/SiO_2 is the lowest (58.29 kJ/mol). Under the same reaction conditions, the activation energy on 10% Sm/SiO_2 is reduced by 25.70 kJ/mol and 41.15 kJ/mol compared with 10% La/SiO_2 and 10% Ce/SiO_2. It has been

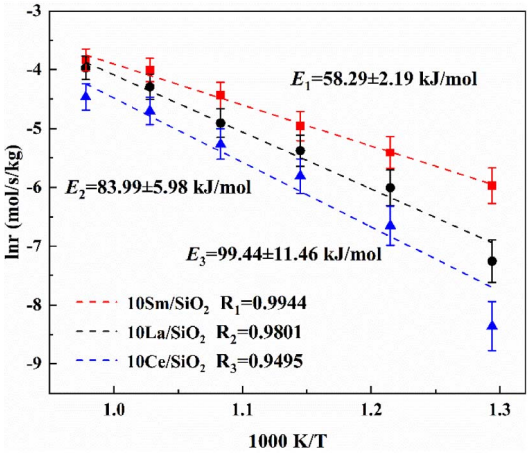

Figure 6. The apparent activation energies on catalysts with different active components.

proved again that 10% Sm/SiO_2 has the best catalytic activity.

In summary, the lanthanide metals Sm and La have good selective catalytic activity for the oxidative dehydrogenation reaction system of CO_2/C_2H_6. Among the three lanthanide metal catalysts, 10% Sm/SiO_2 has the highest catalytic activity, but its C_2H_4 selectivity is lowest. 10% Ce/SiO_2 has the highest C_2H_4 selectivity but its catalytic activity is lowest. 10% La/SiO_2 has both high catalytic activity and high C_2H_4 selectivity; thus La has a more balanced catalytic performance than Sm and Ce. Therefore, La is the most ideal active component. Because of this advantage of La-based catalysts, the effects of different loadings of La on the catalytic activity were further studied.

3.3. *Effect of different loadings of La on reaction performance*

In order to study the effect of different La loadings on the catalytic activity, 5% La/SiO_2, 10% La/SiO_2 and 15% La/SiO_2 were prepared by incipient wetness impregnation method. The catalyst particles (0.25 mL 40–60 mesh) were placed in a quartz tube reactor. The pressure was set to 0.1 MPa, the reaction space velocity was 1200 h^{-1}, and the reaction gas feed ratio was $M_{CO_2/C_2H_6} = 2$. The effects of temperature on C_2H_6 and CO_2 conversion on La/SiO_2 catalysts with different loadings are shown in Figure 7.

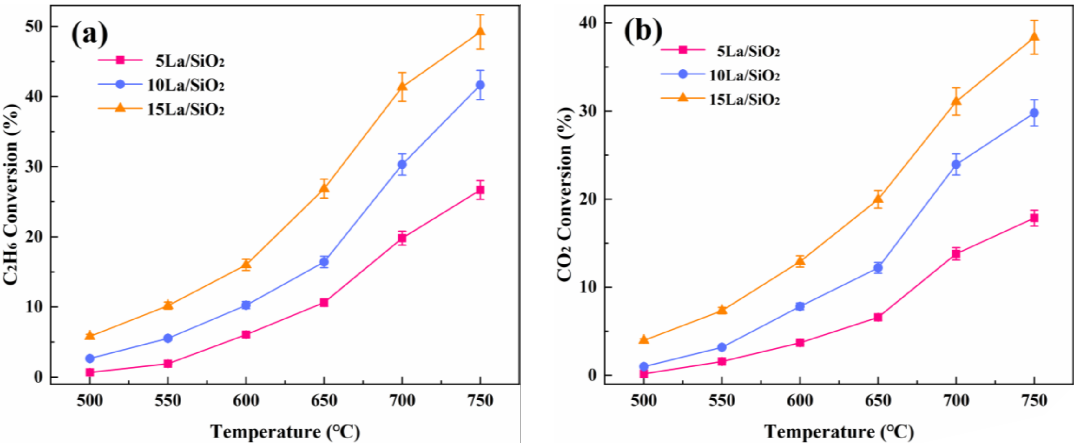

Figure 7. Effect of temperature on C_2H_6 conversion (a) and CO_2 conversion (b) on La/SiO_2 with different loadings.

Figure 7 shows that C_2H_6 and CO_2 conversion on La/SiO_2 with different loadings increase with the increase in reaction temperature. At 650–700 °C, C_2H_6 and CO_2 conversion are higher than its conversion in the lower temperature range. As the loading increases, C_2H_6 and CO_2 conversion increase. Therefore, the catalytic activity for the above catalysts are in decreasing order: 15% La/SiO_2>10% La/SiO_2>5% La/SiO_2. It can be inferred that under the above three loadings, there is no serious active component accumulation or large particle lanthanum oxide crystal on the surface of the catalyst. This conclusion can be confirmed in the catalyst characterization (XRD, EDS and SEM).

Figure 8 shows that CO and CH_4 selectivity on La/SiO_2 with different La loadings increase with the increase in temperature. More importantly, CO and CH_4 selectivity increase with the increase in loadings . Therefore, the increase of loadings of La is conducive to the generation of by-products.

Figure 9 shows that C_2H_4 selectivity on La/SiO_2 with different loadings decreases with the increase in temperature. More importantly, C_2H_4 selectivity decreases with the increase in loading at the same reaction temperature, because the increase in loading promotes the generation of by-products [40,41].

In Figures 8–9, the loading of the catalyst is not as large as possible. For the production of C_2H_4, excessive catalyst loading is detrimental.

The effects of temperature on C_2H_4 yield on La/SiO_2 with different catalyst loadings are shown in Figure 10. C_2H_4 yield on the La/SiO_2 with the above loadings increases with the increase in reaction temperature. More importantly, C_2H_4 yield increases with an increase in loading under the same temperature conditions. La does not show a decrease in C_2H_4 yield as the loading increases, because it still maintains a good dispersion state on the carrier when the loading is 15%. Compared to 10% La/SiO_2, it has more available active sites. It can be further explained that La has good dispersion. This conclusion can be confirmed in the catalyst characterization (XRD, EDS and SEM).

Reducing the activation energy can effectively reduce the temperature required for the reaction, and make the catalytic reaction easier. Therefore, it can achieve the purpose of reducing energy consumption and provide a new way for carbon dioxide absorption [52,53]. The apparent activation energies on La/SiO_2 with different loadings are shown in Figure 11.

Figure 11 shows that the activation energies on La/SiO_2 with different loadings for the catalytic reaction of CO_2/C_2H_6 are in increasing order: 15% La/SiO_2<10% La/SiO_2<5% La/SiO_2; the results are consistent with the previous catalytic activity experiments. The activation energy of the catalytic reaction for 15% La/SiO_2 is the lowest at E = 57.85 kJ/mol. Under the same reaction conditions, the activation energy on 15% La/SiO_2 is reduced by 25.17 kJ/mol and 48.75 kJ/mol compared with 10% La/SiO_2 and 5% La/SiO_2, which prove that

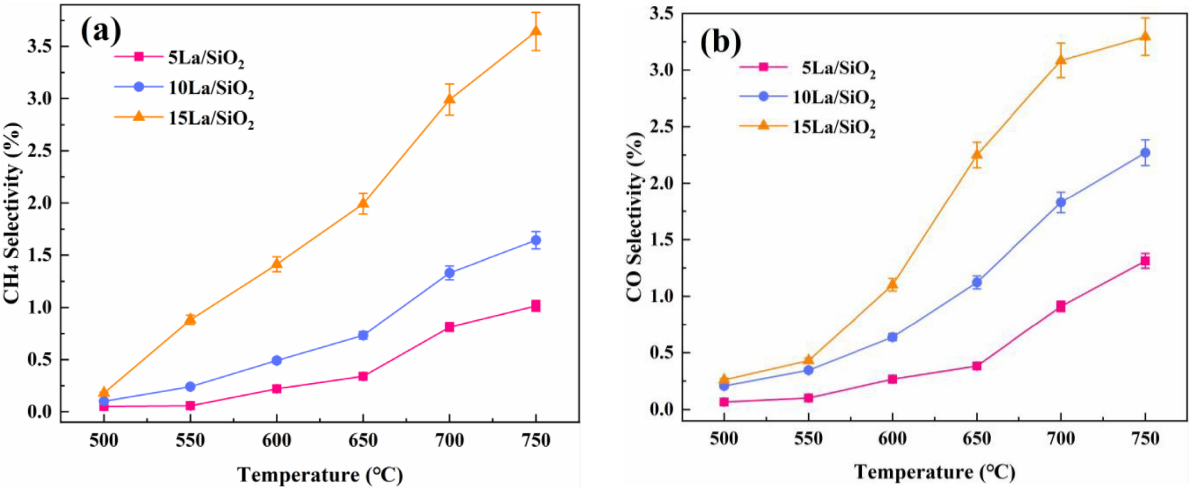

Figure 8. Effect of temperature on CH_4 selectivity (a) and CO selectivity (b) on La/SiO_2 with different loadings.

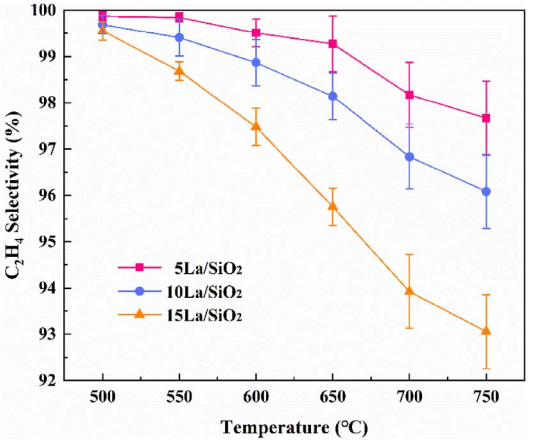

Figure 9. Effect of temperature on C_2H_4 selectivity on La/SiO_2 with different loadings.

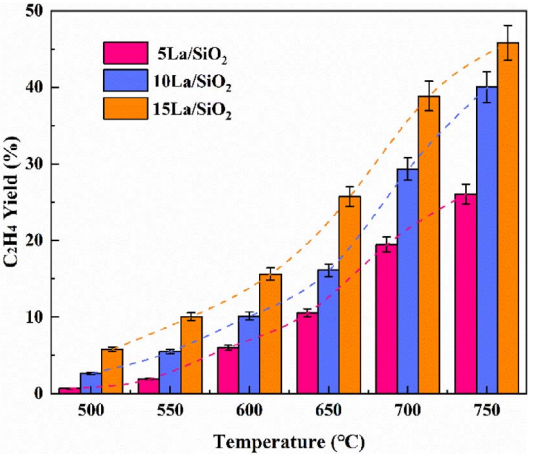

Figure 10. Effect of temperature on C_2H_4 yield on La/SiO_2 with different loadings.

15% La/SiO_2 has the best catalytic activity, the oxidative dehydrogenation of C_2H_6 on 15% La/SiO_2 is most likely to occur, and the reaction rate is the largest. In summary, 15% La/SiO_2 has the best catalytic activity.

3.4. *Microstructure characterization and reaction activity analysis of La-loaded catalysts with different loadings*

Combined with the conclusions obtained from the catalytic activity experiments, we proceeded to study the effect of La/SiO_2 with different loadings on the catalytic activity in the perspective of microstructure. XRD, EDS and SEM were used to characterize the catalysts in this section.

In order to study the crystal phase size of the surface of La/SiO_2 catalyst with different loadings, 5% La/SiO_2, 10% La/SiO_2 and 15% La/SiO_2 were studied by XRD. The XRD images are shown in Figure 12.

In Figure 12, when the loadings of La are 5% and 10%, the diffraction peak of lanthanum oxide crystal does not appear, indicating lanthanum oxides are

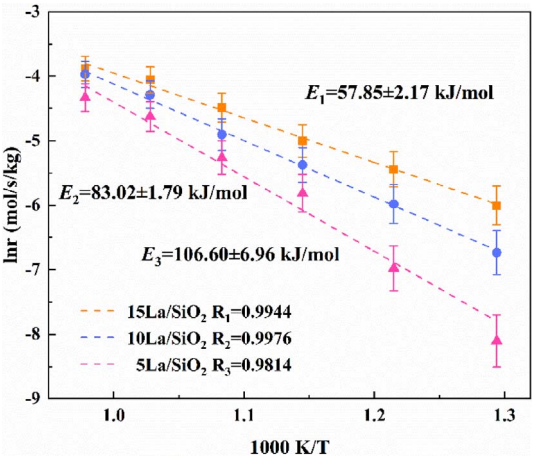

Figure 11. The apparent activation energies on La/SiO_2 with different loadings.

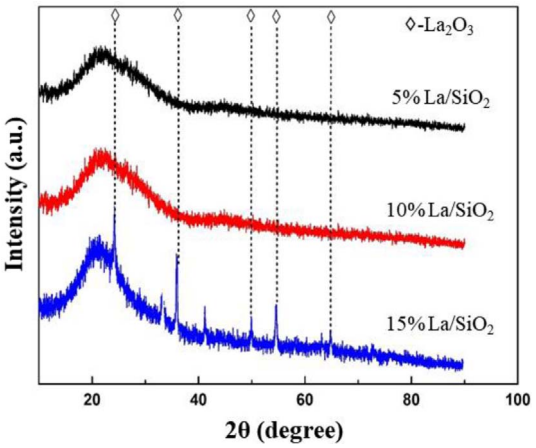

Figure 12. XRD images of La/SiO_2 with different loadings.

highly dispersed on the surface of SiO_2 at the current loading. When the loading of La is increased to 15%, a weak diffraction peak appears; it shows that the lanthanum oxides are excessive and cannot be uniformly dispersed on the surface of the carrier. The peak positions are about 25°, 37°, 50°, 55° and 63°. It indicates that lanthanum oxide crystals begin to appear on the catalyst surface. Combined with the conclusion: 15% La/SiO_2>10% La/SiO_2>5% La/SiO_2; it indicates that the best loading of La/SiO_2 is between 10% and 15%.

In order to further explain that 15% La/SiO_2 has the best catalytic activity among the three loadings, 5% La/SiO_2, 10% La/SiO_2 and 15% La/SiO_2 were studied by SEM and EDS. EDS images of La/SiO_2 with different loadings are shown in Figure 13. SEM images of catalysts with different loadings of La magnified 50 times and 100 times are shown in Figure 14.

In Figure 13, the blue circle indicates the surface of the carrier is not utilized by the lanthanum oxide. The red circle indicates the lanthanum oxides are agglomerated. When the loadings are 5% and 10%, lanthanum oxides can be uniformly distributed on the surface of the carrier, but a large amount of surface area of SiO_2 are not fully utilized (the area drawn by the blue circle). When the loading reaches 15%, the surface of the catalyst is fully utilized by lanthanum oxides and a small amount of aggregation begins to appear (the area drawn by the red circle).

In Figure 14, at the same magnification, most of the lanthanum oxide particles on the 5% La/SiO_2 and 10% La/SiO_2 are relatively small; there is no obvious aggregation. The lanthanum oxides can be well dispersed on the surface of the carrier. The lanthanum oxide particles on 15% La/SiO_2 show a slightly higher degree of growth and aggregation. At this point, the lanthanum oxide particles on the surface of the carrier are still in a relatively good distribution state. According to the experimental results, 15% La/SiO_2 still has high catalytic activity; it indicates that the loading of 15% is only slightly overloaded for La/SiO_2, but does not affect the catalytic performance seriously. Compared with 10% La/SiO_2, 15% La/SiO_2 makes better use of the surface area of the catalyst and has higher catalytic activity. The conclusion that the best loading is between 10% and 15% is proven again.

4. Conclusion

In this paper, the homogeneous reaction of CO_2/C_2H_6 is the coupling of ethane pyrolysis and hydrogenolysis; it starts at 650°C, and the degree of reaction increases rapidly at 750–800°C. Dehydrogenation has better selectivity than reforming on La/Sm/Ce-based catalysts. Due to strong carbon deposition resistance and more oxygen vacancies, Sm exhibits the best catalytic activity; its C_2H_6 conversion is 42.75% on 10% Sm/SiO_2 at 700°C, but its C_2H_4 selectivity is lowest (94.58%), because of high CO and CH_4 selectivity. Ce exhibits the best C_2H_4 selectivity, Ce can regulate the catalyst by its high

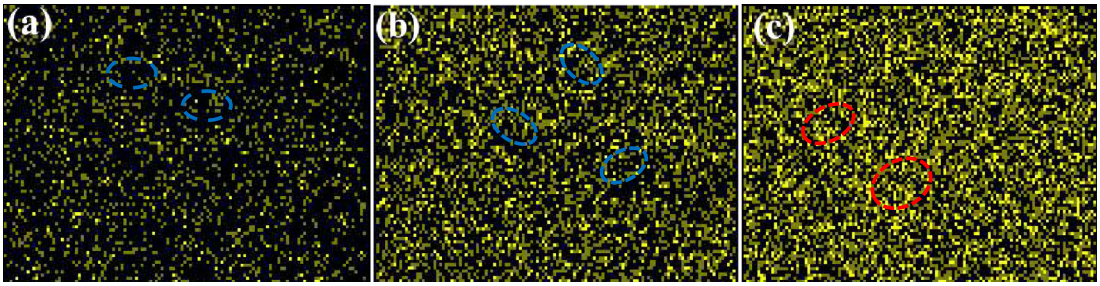

Figure 13. EDS images of La/SiO_2 with different loadings: (a) 5% La/SiO_2, (b) 10% La/SiO_2 and (c) 15% La/SiO_2.

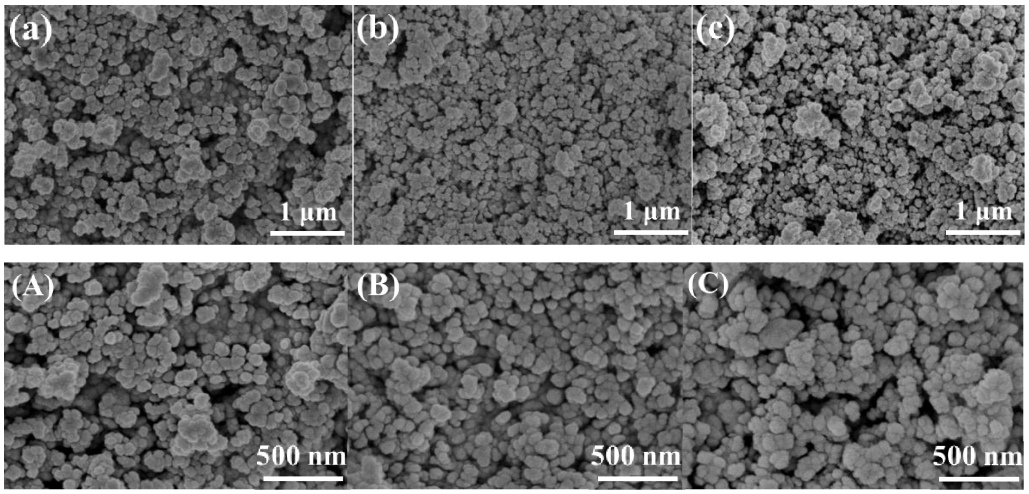

Figure 14. SEM images of La/SiO_2 with different loadings: (a) 5% La/SiO_2 (50 times), (b) 10% La/SiO_2 (50 times), (c) 15% La/SiO_2 (50 times), (A) 5% La/SiO_2 (100 times), (B) 10% La/SiO_2 (100 times) and (C) 15% La/SiO_2 (100 times).

C_2H_4 selectivity because Ce^{4+} promotes the conversion of ethane to ethylene. However 10% Ce/SiO_2 has the lowest catalytic activity; its C_2H_6 conversion is only 42.75% at 700 °C. More importantly, La is the most ideal active component among La, Sm and Ce, catalytic activity and ethylene selectivity are at a high level. The activation energy on 10% La/SiO_2 is 83.99 kJ/mol, C_2H_4 selectivity is 96.84% at 700 °C, its optimal loading is between 10% and 15%. Although 15% La has better catalytic performance than 10% La and 5% La, lanthanum oxides start to aggregate.

In the future work, a catalyst with high catalytic activity and ethylene selectivity is expected to be prepared. Based on the conclusion that Ce-based catalyst has high ethylene selectivity, but its catalytic activity is insufficient, and Sm-based catalyst has high catalytic activity, but its ethylene selectivity is not outstanding, Sm and Ce are co-doped to prepare the lanthanide bimetallic catalyst. The oxidative dehydrogenation characteristics of ethane on the lanthanide bimetallic catalyst are further studied.

Conflicts of interest

The authors declare no competing financial interest.

The manuscript was written through contributions of all authors. All authors have given approval to the final version of the manuscript.

Acknowledgments

This work was supported by the National Natural Science Foundation of China (51876014, 51976019),

and Chongqing Science and Technology Bureau (cstc2018jcyjAX0282).

Supplementary data

Supporting information for this article is available on the journal's website under https://doi.org/10.5802/crchim.4 or from the author. The experimental details including chemicals, materials and instrumentations were given.

References

[1] H. Boukhlouf, A. Barama, R. Benrabaa, J. G. Caballero, A. Lofberg, E. Bordes-Richard, "Catalytic activity in the oxidative dehydrogenation of ethane over Ni and/or Co molybdate catalysts: Synthesis and characterization", *C. R. Chim.*, 2017, **20**, 30-39.

[2] Z. Q. Zhang, L. P. Han, R. J. Chai, Q. F. Zhang, Y. K. Li, G. F. Zhao, Y. Liu, Y. Lu, "Microstructured CeO_2-NiO-Al_2O_3/Ni-foam catalyst for oxidative dehydrogenation of ethane to ethylene", *Catal. Commun.*, 2017, **88**, 90-93.

[3] Z. Q. Zhang, J. Ding, R. J. Chai, G. F. Zhao, Y. Liu, Y. Lu, "Oxidative dehydrogenation of ethane to ethylene: A promising CeO_2-ZrO_2-modified NiO-Al_2O_3/Ni-foam catalyst", *Appl. Catal., A*, 2018, **550**, 151-159.

[4] L. Zhou, S. Y. Hu, D. J. Chen, Y. R. Li, B. Zhu, Y. Jin, "Study on systems based on coal and natural gas for producing dimethyl ether", *Ind. Eng. Chem. Res.*, 2009, **48**, 4101-4108.

[5] L. L. Wu, E. J. M. Hensen, "Comparison of mesoporous SSZ-13 and SAPO-34 zeolite catalysts for the methanol-to-olefins reaction", *Catal. Today*, 2014, **235**, 160-168.

[6] S. A. Al-Sayari, "Catalytic conversion of syngas to olefins over Mn–Fe catalysts", *Ceram. Int.*, 2014, **40**, 723-728.

[7] B. Z. Chu, H. An, T. A. Nijhuis, J. C. Schouten, Y. Cheng, "A self-redox pure-phase M1 MoVNbTeO_x/CeO_2 nanocomposite as a highly active catalyst for oxidative dehydrogenation of ethane", *J. Catal.*, 2015, **329**, 471-478.

[8] J. J. H. B. Sattler, J. Ruiz-Martinez, E. Santillan-Jimenez, B. M. Weckhuysen, "Catalytic dehydrogenation of light alkanes on metals and metal oxides", *Chem. Rev.*, 2014, **114**, 10613-10653.

[9] M. Ermilova, A. Kucherov, N. Orekhova, E. Finashina, L. Kustov, A. Yaroslavtsev, "Ethane oxidative dehydrogenation to ethylene in a membrane reactor with asymmetric ceramic membranes", *Chem. Eng. Process.*, 2018, **126**, 150-155.

[10] L. Ma, C. Qin, S. Pi, H. Cui, "Fabrication of efficient and stable Li_4SiO_4-based sorbent pellets via extrusion-spheronization for cyclic CO_2 capture", *Chem. Eng. J.*, 2020, **379**, 122385.

[11] Y. F. Yan, G. G. Wu, W. P. Huang, L. Zhang, L. X. Li, Z. Q. Yang, "Numerical comparison study of methane catalytic combustion characteristic between newly proposed opposed counter-flow micro-combustor and the conventional ones", *Energy*, 2019, **170**, 403-410.

[12] X. Wang, X. Du, S. Liu, G. Yang, Y. Chen, L. Zhang, X. Tu, "Understanding the deposition and reaction mechanism of ammonium bisulfate on a vanadia SCR catalyst: A combined DFT and experimental study", *Appl. Catal., B*, 2020, **260**, 118168.

[13] L. Kong, J. M. Li, Z. Zhao, Q. L. Liu, Q. Y. Sun, J. Liu, Y. C. Wei, "Oxidative dehydrogenation of ethane to ethylene over Mo-incorporated mesoporous SBA-16 catalysts: The effect of MoO_x dispersion", *Appl. Catal., A*, 2016, **510**, 84-97.

[14] H. B. Zhu, D. C. Rosenfeld, M. Harb, D. H. Anjum, M. N. Hedhili, S. Ould-Chikh, J. M. Basset, "NiMO (M = Sn, Ti, W) catalysts prepared by a dry mixing method for oxidative dehydrogenation of ethane", *ACS Catal.*, 2016, **6**, 2852-2866.

[15] Y. S. Yun, M. Lee, J. Sung, D. Yun, T. Y. Kim, H. Park, K. R. Lee, C. K. Song, Y. Kim, J. Lee, Y. J. Seo, I. K. Song, J. Yi, "Promoting effect of cerium on MoVTeNb mixed oxide catalyst for oxidative dehydrogenation of ethane to ethylene", *Appl. Catal., B*, 2018, **237**, 554-562.

[16] C. A. Gartner, A. C. van Veen, J. A. Lercher, "Oxidative dehydrogenation of ethane: Common principles and mechanistic aspects", *ChemCatChem*, 2013, **5**, 3196-3217.

[17] J. Niu, S. E. Liland, J. Yang, K. R. Rout, J. Ran, D. Chen, "Effect of oxide additives on the hydrotalcite derived Ni catalysts for CO_2 reforming of methane", *Chem. Eng. J.*, 2019, **377**, 119763.

[18] H. Asadi-Saghandi, J. Karimi-Sabet, "Performance evaluation of a novel reactor configuration for oxidative dehydrogenation of ethane to ethylene", *Korean J. Chem. Eng.*, 2017, **34**, 1905-1913.

[19] F. Ayari, R. Charrad, E. Asedegbega-Nieto, M. Mhamdi, G. Delahay, F. Farhat, A. Ghorbel, "Ethane Oxidative Dehydrogenation over ternary and binary mixtures of alkaline and alkaline earth chlorides supported on zeolites", *Microporous Mesoporous Mater.*, 2017, **250**, 65-71.

[20] R. X. Valenzuela, G. Bueno, V. C. Corberan, Y. D. Xu, C. L. Chen, "Selective oxidehydrogenation of ethane with CO_2 over CeO_2-based catalysts", *Catal. Today*, 2000, **61**, 43-48.

[21] R. X. Valenzuela, G. Bueno, A. Solbes, F. Sapina, E. Martinez, V. C. Corberan, "Nanostructured ceria-based catalysts for oxydehydrogenation of ethane with CO_2", *Top. Catal.*, 2001, **15**, 181-188.

[22] A. Beretta, P. Forzatti, "High-temperature and short-contact-time oxidative dehydrogenation of ethane in the presence of Pt/Al_2O_3 and $BaMnAl_{11}O_{19}$ catalysts", *J. Catal.*, 2001, **200**, 45-58.

[23] J. L. Lu, B. S. Fu, M. C. Kung, G. M. Xiao, J. W. Elam, H. H. Kung, P. C. Stair, "Coking- and sintering-resistant palladium catalysts achieved through atomic layer deposition", *Science*, 2012, **335**, 1205-1208.

[24] K. Nakagawa, M. Okamura, N. Ikenaga, T. Suzuki, T. Kobayashi, "Dehydrogenation of ethane over gallium oxide in the presence of carbon dioxide", *Chem. Commun.*, 1998, 1025-1026.

[25] K. Nakagawa, C. Kajita, K. Okumura, N. Ikenaga, M. Nishitani-Gamo, T. Ando, T. Kobayashi, T. Suzuki, "Role of carbon dioxide in the dehydrogenation of ethane over gallium-loaded catalysts", *J. Catal.*, 2001, **203**, 87-93.

[26] R. Koirala, R. Buechel, F. Krumeich, S. E. Pratsinis, A. Baiker, "Oxidative dehydrogenation of ethane with CO_2 over flame-made Ga-loaded TiO_2", *ACS Catal.*, 2015, **5**, 690-702.

[27] O. V. Krylov, A. K. Mamedov, S. R. Mirzabekova, "The regulari-

ties in the interaction of alkanes with CO_2 on oxide catalysts", *Catal. Today*, 1995, **24**, 371-375.

[28] A. Toth, G. Halasi, F. Solymosi, "Reactions of ethane with CO_2 over supported Au", *J. Catal.*, 2015, **330**, 1-5.

[29] K. Nakagawa, C. Kajita, N. Ikenaga, T. Suzuki, T. Kobayashi, M. Nishitani-Gamo, T. Ando, "The role of chemisorbed oxygen on diamond surfaces for the dehydrogenation of ethane in the presence of carbon dioxide", *J. Phys. Chem. B*, 2003, **107**, 4048-4056.

[30] S. B. Wang, K. Murata, T. Hayakawa, S. Hamakawa, K. Suzuki, "Oxidative dehydrogenation of ethane over alkali metal chloride modified silica catalysts", *Energy Fuels*, 2000, **14**, 899-903.

[31] X. J. Shi, S. F. Ji, K. Wang, C. Y. Li, "Oxidative dehydrogenation of ethane with CO_2 over novel Cr/SBA-15/Al_2O_3/FeCrAl monolithic catalysts", *Energy Fuels*, 2008, **22**, 3631-3638.

[32] S. Dangwal, R. C. Liu, S. V. Kirk, S. J. Kim, "Effect of pressure on ethane dehydrogenation in MFI zeolite membrane reactor", *Energy Fuels*, 2018, **32**, 4628-4637.

[33] R. Burch, E. M. Crabb, "Homogeneous and heterogeneous contributions to the catalytic oxidative dehydrogenation of ethane", *Appl. Catal., A*, 1993, **97**, 49-65.

[34] Z. Yang, Y. Lan, Y. Yan, M. Guo, L. Zhang, "Activation pathway of C–H and C–C bonds of ethane by Pd atom with CO_2 as a soft oxidant", *ChemistrySelect*, 2019, **4**, 9608-9617.

[35] V. N. Snytnikov, T. I. Mishchenko, V. N. Snytnikov, S. E. Malykhin, V. I. Avdeev, V. N. Parmon, "Autocatalytic gas-phase dehydrogenation of ethane", *Res. Chem. Intermed.*, 2012, **38**, 1133-1147.

[36] V. N. Snytnikov, T. I. Mishchenko, V. N. Snytnikov, O. P. Stoyanovskaya, V. N. Parmon, "Autocatalytic gas-phase ethane dehydrogenation in a wall-less reactor", *Kinet. Catal.*, 2010, **51**, 10-17.

[37] L. Y. Xu, J. X. Liu, H. Yang, Y. Xu, Q. X. Wang, L. W. Lin, "Regeneration behaviors of Fe/Si_2 and Fe–Mn/Si_2 catalysts for C_2H_6 dehydrogenation with CO_2 to C_2H_4", *Catal. Lett.*, 1999, **62**, 185-189.

[38] Y. Xu, V. C. Corberan, "CeO_2: an active and selective catalyst for the oxidative dehydrogenation of ethane with CO_2", *Prog. Nat. Sci.: Mater. Int.*, 2000, **10**, 22-26, http://cas-ir.dicp.ac.cn/handle/321008/138732.

[39] X. J. Shi, S. F. Ji, K. Wang, C. Y. Li, "Oxidative dehydrogenation of ethane over ce-based monolithic catalysts using CO_2 as oxidant", *Catal. Lett.*, 2008, **126**, 426-435.

[40] S. S. Sigaeva, E. A. Anoshkina, A. R. Osipov, V. L. Temerev, D. A. Shlyapin, A. V. Lavrenov, "Ethane pyrolysis on Al_2O_3, ZrO_2, SiO_2 oxides supported on fechral under conditions of resistive heating", *AIP Conf. Proc.*, 2019, **2143**, 020049.

[41] T. A. Bugrova, V. V. Dutov, V. A. Svetlichnyi, V. C. Corberan, G. V. Mamontov, "Oxidative dehydrogenation of ethane with CO_2 over CrO_x catalysts supported on Al_2O_3, ZrO_2, CeO_2 and $Ce_xZr_{1-x}O_2$", *Catal. Today*, 2019, **333**, 71-80.

[42] T. Q. Lei, C. X. Miao, W. M. Hua, Y. H. Yue, Z. Gao, "Oxidative dehydrogenation of ethane with CO_2 over Au/CeO_2 nanorod catalysts", *Catal. Lett.*, 2018, **148**, 1634-1642.

[43] E. M. Kennedy, N. W. Cant, "Comparison of the oxidative dehydrogenation of ethane and oxidative coupling of methane over rare earth oxides", *Appl. Catal.*, 1991, **75**, 321-330.

[44] D. D. He, D. K. Chen, H. S. Hao, J. Yu, J. P. Liu, J. C. Lu, G. P. Wan, S. F. He, K. Z. Li, Y. M. Luo, "Enhanced activity and stability of Sm-doped HZSM-5 zeolite catalysts for catalytic methyl mercaptan (CH3SH) decomposition", *Chem. Eng. J.*, 2017, **317**, 60-69.

[45] Z. C. Han, Q. B. Yu, Z. J. Xue, K. J. Liu, Q. Qin, "Sm-doped manganese-based Zr–Fe polymeric pillared interlayered montmorillonite for low temperature selective catalytic reduction of NO_x by NH_3 in metallurgical sintering flue gas", *RSC Adv.*, 2018, **8**, 42017-42024.

[46] D. D. He, H. S. Hao, D. K. Chen, J. P. Liu, J. Yu, J. C. Lu, F. Liu, G. P. Wan, S. F. He, Y. M. Luo, "Synthesis and application of rare-earth elements (Gd, Sm, and Nd) doped ceria-based solid solutions for methyl mercaptan catalytic decomposition", *Catal. Today*, 2017, **281**, 559-565.

[47] S. Sharma, S. Hilaire, J. M. Vohs, R. J. Gorte, H. W. Jen, "Evidence for oxidation of ceria by CO_2", *J. Catal.*, 2000, **190**, 199-204.

[48] H. X. Dai, C. F. Ng, C. T. Au, "$SrCl_2$-promoted REO_x (RE = Ce, Pr, Tb) catalysts for the selective oxidation of ethane: A study on performance and defect structures for ethene formation", *J. Catal.*, 2001, **199**, 177-192.

[49] S. Ogo, K. Iwasaki, K. Sugiura, A. Sato, T. Yabe, Y. Sekine, "Catalytic oxidative conversion of methane and ethane over polyoxometalate-derived catalysts in electric field at low temperature", *Catal. Today*, 2018, **299**, 80-85.

[50] M. V. Martinez-Huerta, G. Deo, J. L. G. Fierro, M. A. Banares, "Changes in ceria-supported vanadium oxide catalysts during the oxidative dehydrogenation of ethane and temperature-programmed treatments", *J. Phys. Chem. C*, 2007, **111**, 18708-18714.

[51] Z. H. Xie, B. H. Yan, L. Zhang, J. G. G. Chen, "Comparison of methodologies of activation barrier measurements for reactions with deactivation", *Ind. Eng. Chem. Res.*, 2017, **56**, 1360-1364.

[52] Z. E. Zhang, Y. F. Yan, L. Zhang, Y. X. Chen, J. Y. Ran, G. Pu, C. L. Qin, "Theoretical study on CO_2 absorption from biogas by membrane contactors: Effect of operating parameters", *Ind. Eng. Chem. Res.*, 2014, **53**, 14075-14083.

[53] X. Li, L. Zhang, Z. Yang, P. Wang, Y. Yan, J. Ran, "Adsorption materials for volatile organic compounds (VOCs) and the key factors for VOCs adsorption process: A review", *Sep. Purif. Technol.*, 2019, 116213.